International Journal of Automotive Technology, Vol. 15, No. 2, pp. 191−201 (2014)
DOI 10.1007/s12239−014−0021−y

pISSN 1229−9138/ eISSN 1976−3832

DESIGN OF A COMPRESSOR-POWER-BASED EXHAUST MANIFOLD PRESSURE ESTIMATOR FOR DIESEL ENGINE AIR MANAGEMENT

H. JIN, S. CHOI* and S. KIM

Mechanical Engineering, KAIST, Daejeon 305-701, Korea

(Received 26 October 2013; Revised 30 November 2013; Accepted 31 December 2013)

ABSTRACT−In accordance with the development of hardware configurations in diesel engines, research on model-based control for these systems has been conducted for years. To control the air management system of a diesel engine, the exhaust manifold pressure should be selected as one of the control targets due to its internal dynamic stability and its physical importance in model-based control. However, it is difficult to measure exhaust pressure using sensors due to gas flow oscillation in the exhaust manifold in a reciprocated diesel engine. Moreover, the sensor is too costly to be equipped on production engines. Hence, the estimation strategies for exhaust manifold pressure have been regarded as a primary issue in diesel engine air management control. This paper proposes a new estimation method for determining the exhaust manifold pressure based on compressor power dynamics. With its simple and robust structure, this estimation leads to improved control performance compared with that of general observers. To compensate for the compressor efficiency error that varies with turbine speed, some correction maps are adopted in the compressor power equation. To verify the control system performance with the new estimator, a HiLS (hardware in the loop simulation) of the NRTC mode is performed. Experimental verification is also conducted using a test bench for the C1-08 mode.

KEY WORDS : HP-EGR VGT diesel engine model, Exhaust manifold pressure observer, Compressor power, Model-based sliding mode control, HiLS (hardware in the loop simulation)

NOMENCLATURE

EGR	: exhaust gas recirculation
VGT	: variable geometry turbocharger
MAP	: manifold absolute pressure sensor
MAF	: mass air flow sensor
A_{EGR}	: egr valve effective area, [m^2]
F_i	: air fraction in intake manifold, [-]
F_x	: air fraction in exhaust manifold, [-]
F_e	: air fraction in cylinder, [-]
m_i	: intake manifold mass, [kg]
m_x	: exhaust manifold mass, [kg]
N_e	: engine speed, [rpm]
N_{tc}	: turbocharger rotational speed, [rpm]
p_a	: ambient pressure, [kpa]
p_i	: intake manifold pressure, [kpa]
P_x	: exhaust manifold pressure, [kpa]
P_c	: compressor power, [kw]
P_t	: turbine power, [kw]
R_a	: specific gas constant, [kj/kg·k]
C_p	: specific heat at constant pressure [kj/kg·k]
T_a	: ambient temperature, [k]
T_i	: intake manifold temperature, [k]
T_x	: exhaust manifold temperature, [k]
T_e	: engine out temperature, [k]
T_{ci}	: intercooler outlet temperature, [k]
τ_{tc}	turbine to compressor power transfer time constant (turbocharger time constant), [s]
J_t	: turbine inertia, [$kg{\cdot}m^2$]
V_i	: volume of intake manifold, [m^3]
V_x	: volume of exhaust manifold, [m^3]
V_d	: total displacement volume, [m^3]
W_{ie}	: mass flow rate from intake manifold to cylinder, [kg/s]
W_{EGR}	: egr mass flow rate, [kg/s]
W_{VGT}	: turbine mass flow rate, [kg/s]
W_{ci}	: mass flow rate from compressor to intake manifold, [kg/s]
W_f	: injected fuel mass flow into cylinder, [kg/s]
η_{vol}	: volumetric efficiency, [-]
λ_1, λ_2	: model uncertainties bounded gains, [-]
η_c	: compressor efficiency, [-]
η_t	: turbine efficiency, [-]
η_m	: turbocharger mechanical efficiency, [-]
γ	: specific heat ratio

1. INTRODUCTION

Exhaust gas regulations are gradually improving to reduce NOx and Particulate Matter (PM) in diesel engines. Regarding USA environmental rules, the non-road diesel

**Corresponding author.* e-mail: sbchoi@kaist.ac.kr

engine is faced with regulations that began at Tier 1 in 1996 and will escalate to Tier 4 final in 2014 under the Environmental Protection Agency (EPA). Tier 4 final regulations suggest that NOx and PM be reduced by 96% compared to Tier 1 levels, making it more difficult to manage emission boundaries.

To counteract emissions regulations, precise diesel engine control methods are required for the development of engine configurations. General issues related to the control and modeling of engines have been investigated in (Kao *et al*., 1995; Moskwa and Hedrick, 1992; Zeng, 1999). Furthermore, engineers and scientists can easily study the engine system due to the development of software for engine system simulations (Inman and Sara, 2002; Brian *et al*., 2004). With respect to air management systems, nonlinear properties, such as the coupling effect between the exhaust gas recirculation (EGR) and the variable geometry turbine (VGT), have been analyzed via a variety of mathematical approaches to promote the development of model-based control (Jung, 2003; Bengea *et al*., 2002; Pfeifer *et al*., 2002; Ammann *et al*., 2003; Shamma and Athans, 1991). For the single-loop EGR (HP EGR) and VGT system, a 3rd-order reduced model has been designed mathematically to represent the primary dynamic properties of the actual system and has been validated in many papers (Zheng, 1999; Jung, 2003; Kullkarni *et al*., 1992).

Recently, such a model-based control concept has been expanded to the latest engine configurations, including dual-loop EGR systems (Gautier *et al*., 2009; Olivier and Philippe, 2009; Park *et al*., 2010; Galindo *et al*., 2009). Moreover, modern control skills, such as the adaptation and state observer design, have been incorporated into the control algorithm to enhance engine performance (Storset *et al*., 2000; Stefanopoulou, 2004; Wang, 2008; Swartling, 2005). Regarding the control algorithm itself, the exhaust manifold pressure estimation or measurement method is one of the main issues for developing model-based control. The exhaust pressure value must be known for control because its value is the dominant influence not only for the power dynamics of a turbocharger but also for the main flow dynamics, such as the EGR and turbine flows. Moreover, the exhaust manifold pressure must be one of the control states to guarantee the stability of the internal dynamics in model-based control (Upadhyay, 2001). However, the exhaust pressure is difficult to measure due to unfavorable conditions, such as the high pressure, temperature and pulsation of the engine combustion (Fredriksson and Egardt, 2002; Lee, 2012; Castillo, 2013). The price of sensors is sufficiently expensive to render them unsuitable for production engines.

In estimation methods of the exhaust pressure, observer algorithms have been suggested (Fredriksson and Egardt, 2002; Lee, 2012). However, upon analysis of the observer form, there are some structural problems that make the performance of the observers vulnerable to model uncertainties. For example, the model of a diesel air management system uses inverse models of the orifice equation (describing the behavior of the flows controlled by valves or throttles, such as EGR and VGT flows), which converts the commands of the flows into the corresponding valve positions. Uncertainties in the inverse model cause abnormal observer behavior. As a result, these uncertainties ruin the control performance, which will be discussed in detail below. To solve the chronic problems related to the observer, this paper proposes a new exhaust pressure estimation method that models uncertainties and is simple and robust. This estimation method uses information about the compressor power dynamics rather than other pressures or flow dynamics, in contrast to exisiting approaches.In the design process, the exhaust pressure is treated as a time-varying parameter, not a state parameter, which results in simple calculations. Most importantly, complicated analysis of the global observer criterion in nonlinear observer-based controllers is no longer needed.

Additionally, partial modified turbine and compressor maps are considered to compensate for the modeling errors associated with the efficiency values. With regard to the compressor map, further corrective work is also completed to provide a more accurate estimation.

The model-based controller is a sliding-mode controller, which is a representative robust controller in a nonlinear system. The process of control design, based on the 3rd order engine model, is based on a previous paper (Upadhyay, 2001).

To validate the control performance of the exhaust pressure estimator, both a HiLS (hardware in the loop simulation) and test bench experiments are performed. The HiLS system is composed of a valid engine model and Rapid Control Prototyping (RCP) equipment. Real ECU is connected to LABCAR and RCP by a Controller Area Network (CAN). The test mode is a Nonroad Transient Cycle (NRTC) that is used for verification of the system in transient states. Additionally, experimental verifications are conducted for the C1-08 mode using the test bench. The experimental results show that by using the new estimator, the control performance and robustness of the system are highly enhanced. This paper is organized as follows. In section two, the main model equations of the diesel engine air management system, which is used as a plant model in the HiLS, are introduced. In section three, the design process of the model-based-sliding-mode control, with the compressor flow and the exhaust pressure as the output, is described. In section four, the new exhaust pressure estimator, based on the compressor power and efficiency map design, is introduced.

Overall control performance results and analysis are shown in section five. Finally, we provide a discussion of

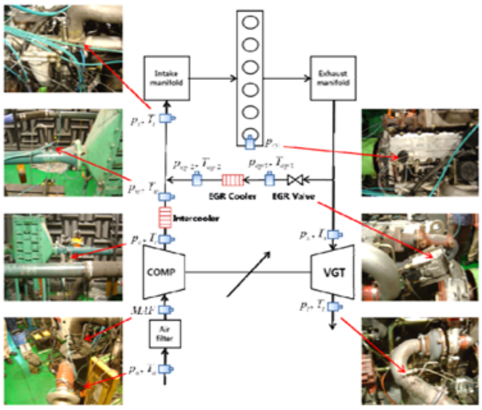

Figure 1. Diesel engine model and test bench description.

the results and conclusions in section six.

2. MEAN VALUE DIESEL ENGINE MODELING

The engine model is implemented based on a heavy-duty 6000cc diesel engine equipped with an HP EGR and VGT system. Considering the thermodynamic properties of adiabatic air flow, the mean value model of the air management system is implemented and validated via test bench experiments. Additionally, a filling and emptying method in which all sub-systems of the engine are represented as a series of control volumes is utilized. The model diagram of the air management system is presented in Figure 1. The system is composed of six mechanical parts: an intake manifold, cylinders, an exhaust manifold, an EGR valve, a compressor, and a turbine.

The mathematical model of the engine configured in Figure 1 is described in equations (1) – (7). The mass flow conservation law is used to derive the flow dynamics represented in equations (1) and (2) (Kao *et al.*, 1995).

$$\frac{dm_i}{dt} = W_{ci} + W_{EGR} - W_{ie} \tag{1}$$

$$\frac{dm_x}{dt} = W_{ie} + W_f - W_{EGR} - W_{VGT} \tag{2}$$

In equations (3) and (4), the gas fraction dynamics are derived from the oxygen concentration of the control volumes and the mass conservation condition (Kao *et al.*, 1995; Moskwa and Hedrick, 1992).

$$\dot{F}_i = \frac{W_{EGR}(F_x - F_i) - F_i W_{ci}}{m_i} \tag{3}$$

$$\dot{F}_x = \frac{W_{ie}(F_e - F_x) - (W_{ie} + W_f)(F_i - F_x)}{m_x} \tag{4}$$

Intake and exhaust manifold dynamics are described by equations (5) and (6) based on the ideal gas law with gas mass flow (Kao *et al.*, 1995; Moskwa and Hedrick, 1992).

$$\dot{p}_i = \frac{\gamma R}{V_i}(T_{ci} W_{ci} + T_x W_{EGR} - T_{ie} W_{ie}) \tag{5}$$

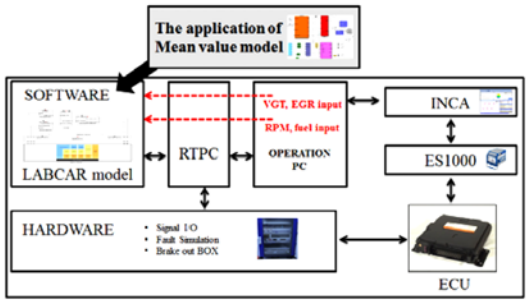

Figure 2. HiLS system diagram.

$$\dot{p}_x = \frac{\gamma R}{V_x}(T_e(W_{ie} + W_f) - T_x(W_{EGR} + W_{VGT})) \tag{6}$$

The compressor power dynamics are expressed as in equation (7) using the turbine power and total system efficiency (Upadhyay, 2001).

$$\frac{dP_c}{dt} = \frac{1}{\tau_{tc}}(-P_c + \eta_m P_t) \tag{7}$$

Where $P_t \approx \eta_m \eta_t C_p T_x \left(1 - \left(\frac{p_a}{p_x}\right)^{\mu}\right) W_{VGT}$

P_t is the power delivered by the turbine, and P_c is the power generated by the compressor.

These modeling methods have been described in more detail (Kao *et al.*,1995; Moskwa and Hedrick, 1992; Zeng, 1999; Upadhyay, 2001).

2.1. HiLS System Description

To verify the model and the controller, a HiLS system is implemented. The overall control and verification system is shown in Figure 2. The diesel engine air management system, implemented in Matlab/Simulink, is tuned using real experiments and WAVE simulation. This model is embedded on an RTPC and connected to an ECU via a

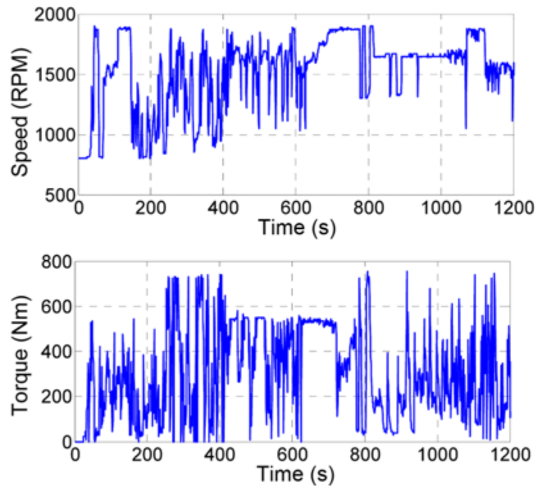

Figure 3. Engine RPM (upper) and torque (lower) trajectories of the NRTC mode.

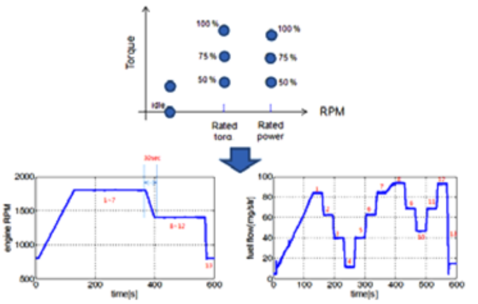

	1	2	3	4	5	6	7	8	9	10	11	12	13
Speed (RPM)	1800							1400					idle
Load (%)	100	75	50	10	50	75	100	100	75	50	75	100	0

Figure 4. C1-08 mode (upper), trajectories of the engine RPM (middle left) and the fuel flow (middle right), and mode procedure (lower).

CAN bus system. The other sub-models of the diesel engine, except for the air management system, such as the fuel injection and valve timing, are implemented in LABCAR. Calibration of the measurement data is conducted by the INCA tool. For controller verification, AUTOBOX is also connected to the RTPC via the CAN bus system.

Total system verification is conducted for the NRTC mode, which is a representative transient driving cycle for mobile non-road diesel engines. The total driving time is approximately 1200 seconds. As shown in Figure 3, the engine RPM and load are independently varied during the entire engine operation. Because of these properties, the NRTC mode is widely known for its function verifying the control performance in transient situations.

2.2. Test Mode Description

To verify the system experimentally with a test bench under steady state conditions, the C1-08 test mode, with fixed RPM and load operating points, is adopted. In the test bench, the intake pressure, compressor flow, RPM and fuel flow data are received from the CAN signals, which are connected to the engine cell ECU and sensors. Controllers are imbedded in AUTOBOX, which is connected to the CAN bus system. The C1-08 mode is depicted in Figure 4. The rated torque and RPM are set at 1400 and 1800 RPM, respectively. Each steady state mode is maintained for 20 seconds. Mode transition was conducted with a linear shape. Each steady mode has a transition time of 5 seconds. The RPM transition between modes 7 and 8 is activated for 30 seconds.

3. MULTIVARIABLE SLIDING MODE CONTROLLER

The control-oriented model of this paper is the well-known 3rd order model for the air management system-of a diesel engine equipped with a VGT and HP-EGR system. The 3rd order model is as follows.

$$\dot{p}_i = k_i\left(\frac{\eta_c}{C_pT_a}\frac{P_c}{\left(\left\{\frac{p_i}{p_a}\right\}^{\mu}-1\right)}+W_{EGR}-k_ep_i\right) \tag{8}$$

$$\dot{p}_x = k_2(k_ep_i+W_f-W_{EGR}-W_{VGT}) \tag{9}$$

$$\dot{P}_c = \frac{1}{\tau}\left(-P_c+\eta_m\eta_tC_pT_x\left(1-\left(\frac{p_a}{p_x}\right)^{\mu}\right)W_{VGT}\right) \tag{10}$$

Where $k_1=\frac{RT_i}{V_i}, k_e=\frac{\eta_e N V_d}{120RT_i}, k_2=\frac{RT_i}{V_x}$.

This model comprises three dynamics: the intake, exhaust manifold pressure and compressor power dynamics. The 3rd order model is obtained from the full order models (1) ~ (7) with the following assumptions.

- Air fraction states, which are difficult to measure and are not directly coupled with other dynamic equations, are ignored.
- Residual gas mass states, which are difficult to measure and to control independently of the intake and exhaust manifold, are ignored.
- Temperature is invariant at the same operating points.

Based on the 3rd order model, a sliding mode controller is designed using the multivariable input-output linearization method (Upadhyay, 2001). Upon analysis of a variety of output sets, the compressor flow and exhaust pressure states are chosen as the control states because they are appropriate for state error regulation problems. Other output cases of controllers and their internal dynamics stabilities are analyzed in (Upadhyay, 2001). The present paper focuses on exhaust pressure estimation methods. Hence, we will briefly describe the controller design process in the next section.

3.1. Control Design with the Compressor Flow and the Exhaust Manifold Pressure as the Output Set

In the control with this output set, it is shown that the internal dynamics are stable, and the resulting EGR flow can satisfy emissions regulations. The siding surfaces are designed as follows:

$$S_1 = p_x - p_x^d \tag{11}$$

$$S_2 = W_{ci} - W_{ci}^d \tag{12}$$

Differentiating S_1 and S_2

$$\begin{aligned}\dot{S}_1 &= k_{2\_model}\left(k_ep_i+W_{f\_model}\right)-k_{2\_model}u_1\cdots\\ &\quad -k_2u_2+\Delta k_2\left(\Delta k_ep_i+\Delta W_f\right)-\Delta k_2u_1-\Delta k_2u_2\end{aligned} \tag{13}$$

$$\begin{aligned}\dot{S}_2 = &-\frac{1}{\tau_{tc}}\cdot W_{ci} - \alpha_{\text{model}}\left(W_{ci} - k_{e\_\text{model}}p_i\right)\ldots\\ &-\alpha_{\text{model}}u_1 + \beta_{\text{model}}u_2 - \Delta\alpha\left(W_{ci} - \Delta k_e p_i\right)\ldots\\ &-\Delta\alpha u_1 + \Delta\beta u_2\end{aligned} \tag{14}$$

where

$u_1 = W_{EGR}$

$u_2 = W_{VGT}$

$\alpha = k_1 W_{ci}\dfrac{\mu p_i^{\mu-1}}{p_i^{\mu} - p_a^{\mu}}$

$\alpha_{\text{model}} = k_{1\_\text{model}} W_{ci}\dfrac{\mu p_i^{\mu-1}}{p_i^{\mu} - p_a^{\mu}}$

$$\beta = \frac{1}{\tau_{tc}}\cdot\frac{\eta_c\eta_t\eta_m T_x}{T_a}\frac{\left(1-\left(\frac{p_a}{p_x}\right)^{\mu}\right)}{\left(\frac{p_i}{p_a}\right)^{\mu}-1},$$

$$\beta_{\text{model}} = \frac{1}{\tau_{tc}}\cdot\frac{\eta_{c\_\text{model}}\eta_{t\_\text{model}}\eta_{m\_\text{model}}T_x}{T_a}\frac{\left(1-\left(\frac{p_a}{p_x}\right)^{\mu}\right)}{\left(\frac{p_i}{p_a}\right)^{\mu}-1}$$

In equation (13), k_{2_model} is the known modeled portion of k_2, and Δk_2 is the unknown portion with values bounded by δ_1, as described in (15).

$$|\Delta k_2| < \delta_1 \tag{15}$$

In the same manner, α_{model} and β_{model} are the known modeled parts of α and β, and $\Delta\alpha$ and $\Delta\beta$ are the unknown parts with bounded values as follows:

$$|\Delta\alpha| < \delta_2 \tag{16}$$

$$|\Delta\beta| < \delta_3 \tag{17}$$

The control laws u_1 and u_2 that satisfy the $S_1\dot{S}_1 < 0$ and $S_2\dot{S}_2 < 0$ conditions are designed as follows:

$$u_1 = \frac{1}{\alpha_{\text{model}}+\beta_{\text{model}}}\left(\begin{aligned}&k_e p_i\left(\alpha_{\text{model}}+\beta_{\text{model}}\right)+\ldots\\ &\beta_{\text{model}}W_f - W_{c_i}\left(\frac{1}{\tau_{tc}}+\alpha_{\text{model}}\right)\ldots\\ &+\beta_{\text{model}}k_{2\_\text{model}}^{-1}\left(\frac{\eta_1 S_1}{\phi_1}\right)\ldots\\ &+\left(\frac{\eta_2 S_2}{\phi_2}\right)\end{aligned}\right) \tag{18}$$

$$u_2 = \frac{1}{\alpha_{\text{model}}+\beta_{\text{model}}}\left(\begin{aligned}&\left(\alpha_{\text{model}}\right)W_f\ldots\\ &+\left(\alpha_{\text{model}}\right)k_{2\_\text{model}}^{-1}\left(\frac{\eta_1 S_1}{\phi_1}\right)\ldots\\ &+W_{ci}\left(\frac{1}{\tau_{tc}}+\alpha_{\text{model}}\right)-\left(\frac{\eta_2 S_2}{\phi_2}\right)\end{aligned}\right) \tag{19}$$

The positive constants are chosen such that

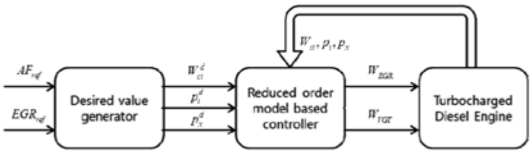

Figure 5. Sliding mode control algorithm.

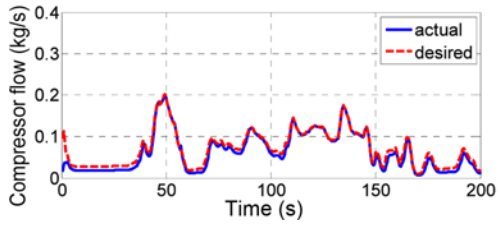

Figure 6. Compressor flow of the sliding mode controller (for the controller verification only, HiLS).

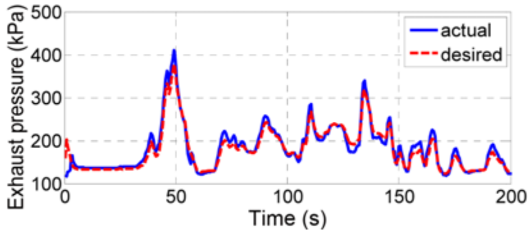

Figure 7. Exhaust pressure of the sliding mode controller (for the controller verification only, HiLS).

$$\delta_1 + c_1 = \eta_1 \tag{20}$$

$$\delta_2 + \delta_3 + c_2 = \eta_2 \tag{21}$$

where c_1 and c_2 are positive constant stability margins. ϕ_1 and ϕ_2 are the error bounds of the first and second surfaces, respectively. The $\dot{p}_{id}$ and $\dot{p}_{xsd}$ terms are omitted because they do not critically affect the system characteristics.

The simulation for verifying the sliding mode controller's performance is conducted for the NRTC mode. To check the tracking performance of the controller closely, the verification is completed for the first 200 seconds of the NRTC mode. The control principle is depicted in Figure 5.

The simulation results of the control targets, compressor flow and exhaust pressure are presented in Figures 6 and 7.

The exhaust pressure values can be obtained directly from the engine model, and the desired reference values are taken from the experimental results of a production engine bench test. Figures 6 and 7 show that the control performances are good, with few model uncertainties between the plant model and the controller reduced-order model.

However, the exhaust pressure must be estimated because the state is not measurable. It is clear that the control performance will deteriorate if estimated values are used rather than the actual plant output values.

4. EXHAUST PRESSURE ESTIMATION

4.1. Conventional Exhaust Pressure Observer

Observer gains are generally designed in consideration of the sensor bandwidth. Moreover, the engine characteristics responding to the controller gains must be analyzed. The 3rd order model-based observer is generally developed as follows:

$$\dot{\hat{p}}_i = k_1\left(\frac{\eta_c}{C_pT_a}\frac{P_C}{\left(\left\{\frac{\hat{p}_i}{p_a}\right\}^{\mu}-1\right)} + W_{EGR} - k_e\hat{p}_i\right)\cdots \\ + L_1(p_i-\hat{p}_i), \tag{22}$$

$$\dot{\hat{p}}_x = k_2(k_e\hat{p}_i + W_f - W_{EGR} - W_{VGT}) + \\ L_2(p_i-\hat{p}_i) + L_3(P_c-\hat{P}_c), \tag{23}$$

$$\dot{\hat{P}}_c = \frac{1}{\tau_{tc}}\left(\begin{array}{c}\dfrac{C_pT_a\left(\left\{\frac{\hat{p}_i}{p_a}\right\}^{\mu}-1\right)}{\eta_c}W_{ci}+\cdots \\ \eta_m\eta_tC_pT_2\left(1-\left(\frac{p_a}{\hat{p}_x}\right)^{\mu}\right)W_{VGT}\end{array}\right) + L_4(P_c-\hat{P}_c), \tag{24}$$

This observer form is based on the Luenberger observer. Each estimated state has the observer gain, L_i, with an estimation error term. The estimated intake pressure (22) is computed from MAP sensor data, p_i. The compressor power can be calculated with high precision from the compressor flow, W_{ci}, which is measured using a MAF sensor. When the observability of this system is determined using the Lie derivative of (22) ~ (24), the rank is found to be three. This result indicates that the system is locally observable. However, it is not easy to tune the observer gains, L_2 and L_3, if the actual exhaust pressure value is unknown. Moreover, the observer system has critical structural problems. The observer-based control scheme is shown in Figure 8.

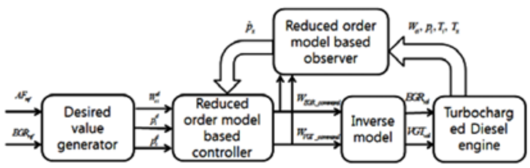

Figure 8. Observer-based controller system scheme.

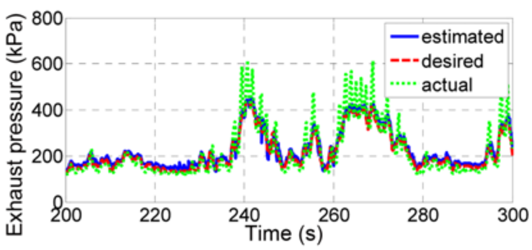

Figure 9. Exhaust pressure of the sliding mode control with an observer based on the 3rd order model (HiLS result).

In contrast to Figure 5, the observer and inverse model blocks are included in Figure 8. The control performance is directly affected by the accuracy of the inverse model. The inverse model has a role in creating the VGT vane and the EGR valve position commands from the controller outputs of the VGT and EGR flows using the orifice equations. Therefore, the uncertainty of the inverse model causes the difference between the actual flow values into the engine and the controller output flow used in the observer.

The controller can be tuned to track the desired exhaust pressure created by the observer. However, the observer and the controller are designed based on the same uncertain engine model. Therefore, there is no guarantee that the estimated exhaust pressure will converge to the actual one. The deviation is dependent on the amount of model uncertainty.

Figure 9 shows that the actual value does not track the desired value well. Instead, the estimated value converges to the desired value as expected above.

Errors are caused by the unmatched conditions between the controller output flows and the actual flows used by the plant, as shown in Figures 10 and 11.

In Figure 10, the controller computes the VGT flow command using the estimated exhaust pressure, which is similar to the desired value. However, the actual VGT flow shows an overshoot and chattering phenomenon at some operating points with a trajectory shape that is quite

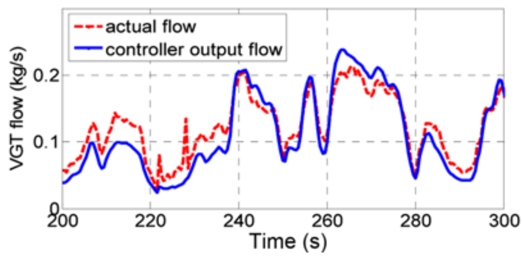

Figure 10. Comparison between the VGT controller output flow and the actual VGT flow (HiLS result).

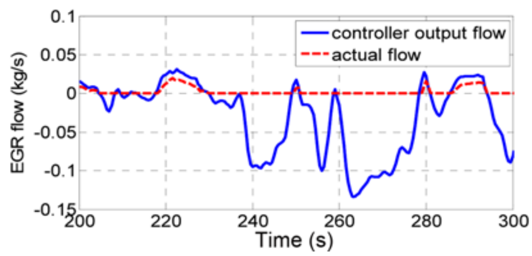

Figure 11. Comparison between the EGR controller output flow and the actual EGR flow (HiLS result).

different from the VGT flow provided by the controller. As shown in Figure 11, due to the inaccurate exhaust pressure values from the observer, the EGR controller output flows have negative values, indicating that the flow is in the reverse direction. However, the actual EGR flow does not exist because the EGR valve is fully closed. These differences between the controller output and actual plant flows disturb the system balance and eventually destroy the control performance.

4.2. Compressor Power Based Exhaust Pressure Estimation

4.2.1. Estimator design

To solve the structural problem and to enhance the robustness of our approach, a compressor power-based exhaust pressure estimation method is proposed. In this estimation method, the exhaust pressure is regarded as a time-varying parameter rather than the control state. Using the compressor power dynamics with the turbine power equation (7), the exhaust pressure can be derived as (25).

$$\hat{p}_x = \frac{p_a}{\left(1 - \dfrac{P_c + \tau_{tc}\dot{P}_c}{\eta_t \eta_m c_p T_x W_{VGT}}\right)^{1/\mu}}, \qquad (25)$$

where $P_c = \dfrac{\left(1-\left(\dfrac{p_i}{p_a}\right)^{\mu}\right) T_a c_p W_{ci}}{\eta_c}$

As noted above, the estimated value is at risk of chattering due to the unexpected VGT controller output flow present in some operating points. To avoid the chattering phenomenon, the VGT flow value is replaced by the sum of the compressor flow and the fuel flow, ($W_{VGT} \approx W_{ci} + W_{fuel}$), which can be measured by the MAF sensor and the fuel flow signal of the ECU, respectively.

The turbine and compressor efficiency can be regarded simply as constant values or calculated from the turbine map data to improve the accuracy.

4.2.2. Turbine efficiency map design

Assuming the turbine efficiency is a constant value does not affect the system stability or robustness; however, it gives rise to estimation errors because the estimator is based on the turbocharger power dynamics. Hence, the efficiency values must be tuned properly, or correction factors are added to the calculation process of (25).

The turbine efficiency is simply updated as a function of the turbine pressure ratio and the VGT vane position. There are several reasons for creating a simple turbine efficiency map without considering the turbine speed (Gamma Technologies GT-SUITE, 2008).

The first reason is that it is not possible to measure actual efficiency values directly, and it is clear that for the ranges of data on the map, extrapolation does not provide reasonable values. The second reason is that the turbine data for extremely high or low pressure ratios are not appropriate for a fitting algorithm. The third reason is that

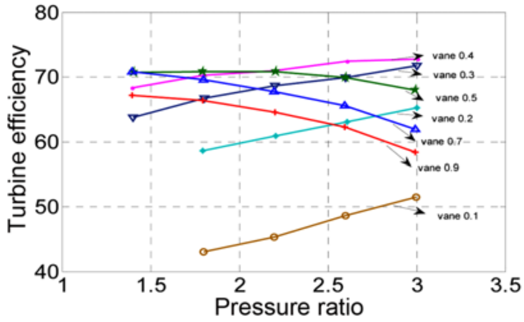

Figure 12. Simplified turbine efficiency map.

the speed line is generally noisy with more than one local maximum efficiency. Thus, measurement of the turbine speed is not practical.

Therefore, turbine efficiency maps using the vane position and the pressure ratio as the input values can be designed, as shown in Figure 12. Except the vane position of 0.1, the majority of the efficiency values are near 60~70%, and the variations of the turbine efficiency values are influenced more by the vane position than by the pressure ratio. Using these map data, the optimal operating points can be easily derived. Moreover, the modifications made to the turbine efficiency play an important role in turbine speed correction when estimating turbine speeds (using the turbocharger power dynamics in the next section).

4.2.3. Compressor efficiency map design

The compressor efficiency value can be determined using the manufacturer's map data. In the design process, analysis of the surge and choke lines must be completed first. The surge line defines the limits of the compressor to compress air at a given speed and compressor ratio. Therefore, when the values of the pressure ratio or the turbine speed are located to the left of the surge line, unstable compressor flow will occur; this instability must be avoided in a turbocharger system. Another undesired operating line is the choke line. Choking of the compressor occurs when the compressor is operating at a low pressure

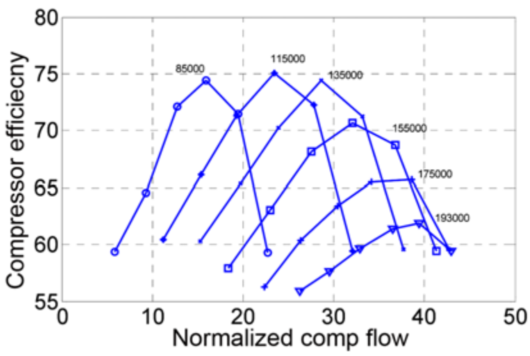

Figure 13. General compressor efficiency map.

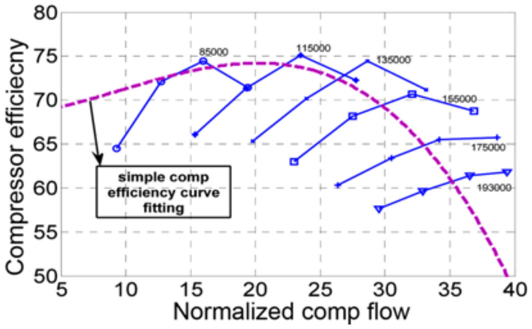

Figure 14. Simplified compressor efficiency map and compressor flow.

ratio and a very high compressor flow. This leads to a significant increase in the flow velocity of the compressor, which can even reach a sonic velocity.

The compressor efficiency can also be obtained from the efficiency map, as shown in Figure 13. Using the surge and choke lines, each compressor efficiency with the same turbine speed has a convex form.

By omitting the impractical points of the surge and choke lines, it is possible to fit the curve with the main operating points using interpolation, as shown in Figure 14.

When this map is used to estimate the exhaust pressure, the exhaust pressure errors are bounded at less than 5-10%, as determined from the test bench data described in section 5. However, we must consider the effects of turbine speed variations on efficiency. When the values of the turbine and compressor power are provided, the corresponding turbine speed can be estimated using (26).

$$\frac{d}{dt}\omega_t = \frac{P_t\eta_m - P_c}{J_t\omega_t} \qquad (26)$$

where η_m is the mechanical efficiency of the turbocharger and J_{tc} is the turbocharger inertia; this information is usually available from the manufacturer.

Using the estimated turbine speed, we can demonstrate the effects of speed variations on the original compressor efficiency map shown in Figure 14. The resulting map,

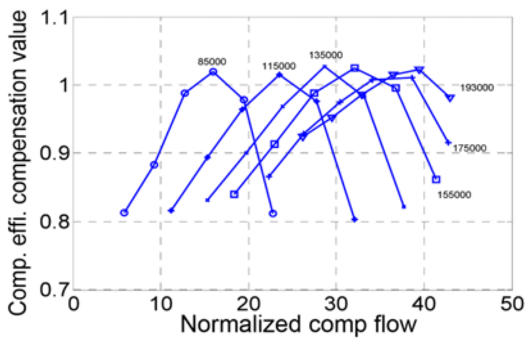

Figure 15. Compressor efficiency value compensation map.

which corrects the simplified compressor efficiency map, is shown in Figure 15.

Then, a corrective map is constructed considering the errors between the actual compressor efficiency data and the simplified curve fit data. Finally, the compressor efficiency compensation values are applied to (25).

The overall process of exhaust pressure estimation is illustrated in Figure 16.

As shown in Figure 16, if a simplified exhaust pressure estimation is desired, the simple method [a] is appropriate. However, if a more accurate exhaust pressure estimation is required, the full model estimator [a]+[b] should be used.

5. VERIFICATION OF THE EXHAUST PRESSURE ESTIMATOR

Applying the estimation method defined in (25) to the sliding mode controller, the exhaust pressure estimation performance is verified experimentally using both a HiLS and a real engine on a test bench for both the transient and steady state tracking profiles.

5.1. HiLS Test

As mentioned in section 4, the conventional exhaust

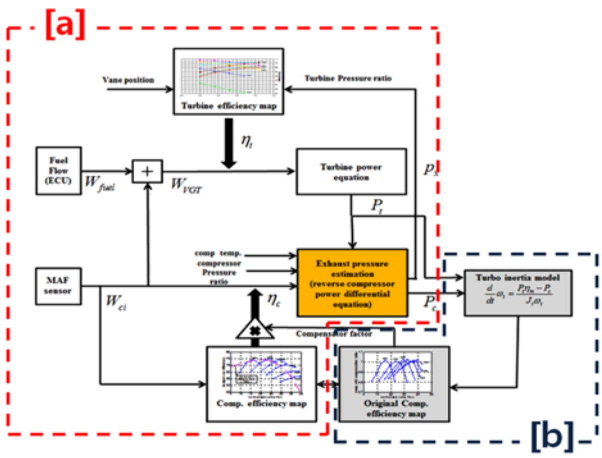

Figure 16. Exhaust pressure estimation diagram ([a] simple method, [b] compressor efficiency error correction method).

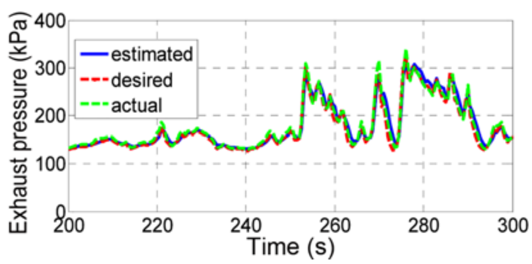

Figure 17. Exhaust pressure estimation using the compressor power equation.

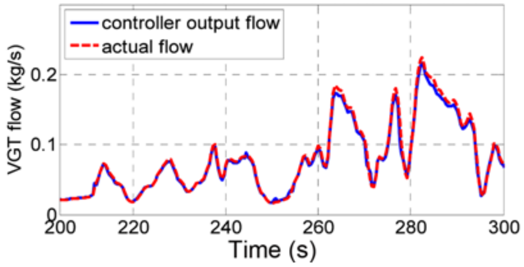

Figure 18. Comparison between the VGT controller output flow and the VGT actual flow (using the compressor power-based exhaust pressure estimation).

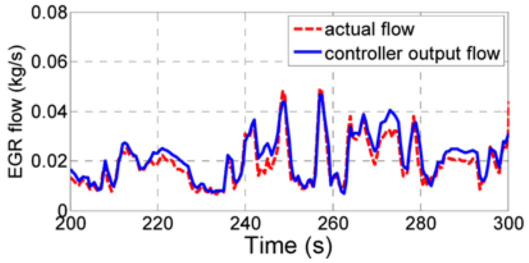

Figure 19. Comparison between the EGR controller output flow and the EGR actual flow (using the compressor power-based exhaust pressure estimation).

pressure observer causes chattering in the actual exhaust pressure value due to the errors between the controller and actual plant flows. To demonstrate the performance improvement, the HiLS test of the controller with the new compressor power-based estimator is performed, as shown in Figures 17 ~ 19.

In Figure 17, the estimated exhaust pressure based on the compressor power tracks the actual exhaust pressure, not the desired value. Compared to Figure 9, Figure 17 shows a significant tracking performance improvement. In Figure 18, the trajectory of the command VGT flows is nearly identical to that of the actual values. In Figure 19, the two EGR flows have nearly the same shapes, with errors in an acceptable range. These results are from enhancement of the overall control system performance. The expected behavior of the VGT and EGR flows ensures acceptable mass flow balances in the exhaust manifold.

To verify the performance of the exhaust pressure estimation under steady state conditions, a test bench experiment is performed using a real engine. The effects of efficiency errors on the estimation results can be seen clearly under steady state conditions. Hence, we must experiment with the conditions to verify the effectiveness of the efficiency corrective maps.

5.2. Test Bench Experiments

The actual exhaust pressure value is measured using a sensor in the engine test bench.

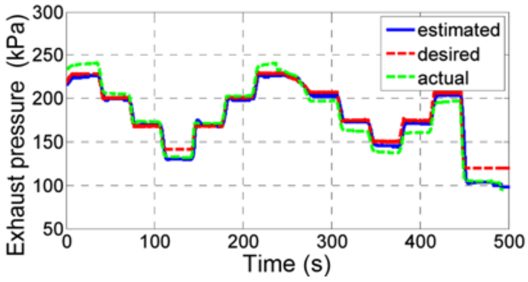

Figure 20. Compressor power-based exhaust pressure estimation without correction factors.

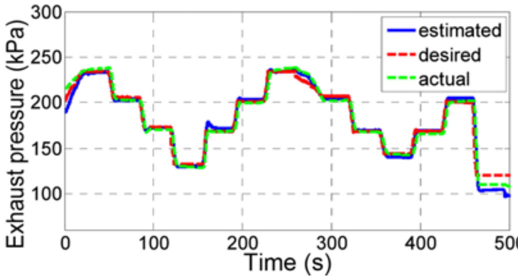

Figure 21. Compressor power-based exhaust pressure estimation with correction factors.

The control results that use the new exhaust pressure estimator, but without the compressor efficiency correction factors, are shown in Figure 20.

In Figure 20, the estimated exhaust pressure follows the actual values without the chattering phenomenon, and the actual values also track the desired values. However, there are some steady state errors at 1800 RPM and the 100% load condition. These are also apparent at 1400 RPM and the 75% load condition. We assume that these steady state errors stem from the efficiency errors. Therefore, the proposed efficiency maps are used for the estimation algorithm instead of the simplified maps. The bench test results using the maps are shown in Figures 21 ~ 23.

Figure 21 shows that the control and estimation performances are enhanced significantly compared to the previous results. The improvement of the estimation

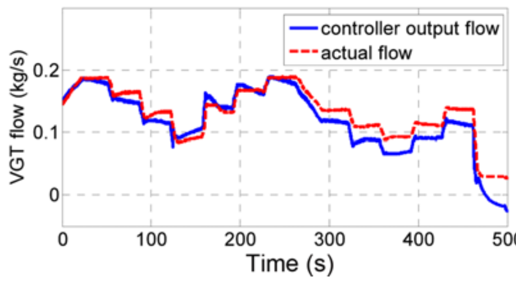

Figure 22. Comparison of the VGT controller output flow and the VGT actual flow (using the correction factors).

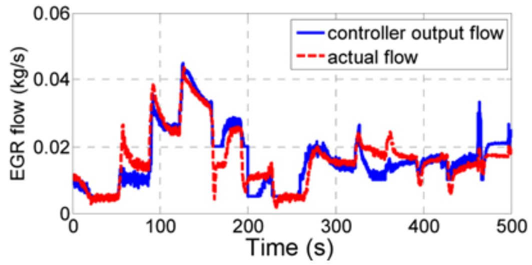

Figure 23. Comparison of the EGR controller output flow and the EGR actual flow (using the correction factors).

performance can be explained by the results of the VGT and EGR flows shown in Figures 22 ~ 23.

These results show that both the VGT and EGR flows follow the controller output flows reasonably well. At operating points between 280 and 450 seconds, there are some steady state errors caused by model uncertainties, such as compressor and turbine efficiency, which are assumed to be constant values. However, these flow errors do not affect the exhaust pressure estimator substantially, which indicates that the exhaust pressure estimator is robust to the model uncertainties.

Figure 23 shows that 5~20% of the EGR rates are maintained for the overall operating points. Considering that the flow is relatively small, it can be assumed that the errors in Figure 23 are acceptable for EGR rate evaluation, thus indicating that accurate estimation of the exhaust pressure enables the engine output torque to track the driver's intention at a high bandwidth, and emissions regulations are met due to proper EGR control.

6. CONCLUSION

This paper investigates an exhaust pressure estimation method for a VGT- and HP-EGR-based diesel engine.

Using the compressor power equation, the exhaust pressure can be estimated with high precision while maintaining robustness. For the conventional observers that are based on a 3rd order model, the estimation accuracy is poor, particularly for transient conditions, due to the model uncertainties, including flow errors. In contrast, the compressor power-based exhaust pressure estimation method is very robust and uses only reliable values acquired from actual sensors, such as the compressor and fuel flows. As expected, this method shows remarkable improvement in estimation accuracy.

Additionally, corrective efficiency maps, which are simplified to be independent of the turbine speeds, are incorporated into the system to compensate for the turbine and compressor dynamics efficiency errors.

In real applications, the compressor power dynamics are rarely used because it is difficult to calculate the compressor power values accurately. The power values are determined from the time-varying values of turbocharger efficiency. These values may need to include turbine speed data.

Hence, an additional corrective map of the compressor efficiency, which includes information about the turbine speed variations, is created. For the corrective map, the turbine speed is estimated from the 1st order lagged model of turbocharger power dynamics.

In conclusion, the exhaust pressure can be estimated with high accuracy and robustness. Therefore, the engine control system using the proposed estimation method can satisfy both control performance specifications and environmental regulation requirements.

ACKNOWLEDGEMENT–This research was supported by the MKE (The Ministry of Knowledge Economy), Korea, under the CITRC (Convergence Information Technology Research Center) support program (NIPA-2013-H0401-13-1009), which is supervised by the NIPA (National IT Industry Promotion Agency).

REFERENCES

Ammann, M. and Fekete, N. P., Guzzella, L. and Glattfelder, A. H. (2003). Model based control of the VGT and EGR in a turbocharged common-rail diesel engines: Theory and passenger car implementation. *SAE Paper No.* 2003-01-0357.

Bengea, S., DeCarlo, R., Corless, M. and Giorgio, R. (2002). A Polytopic System Approach for the Hybrid Control of a Diesel Engine using VGT/EGR. Technical Report. Purdue University.

Brian, D. F. (2004). *Diesel Engine Modeling in WAVE. Pennsylvania State University*. The Graduate School. College of Engineering.

Castillo, F. (2013). Exhaust manifold estimation diesel equipped with a VGT turbocharger. *SAE Paper No.* 2013-01-1752.

Fredriksson, J. and Egardt, B. (2002). Estimating exhaust manifold pressure in a turbocharged diesel engine. *Proc. 2002 IEEE Int. Conf. Control Applications*, **2**, 701−706.

Galindo, J., Climent, H., Guardiola, C. and Domenech, J. (2009). Strategies for improving the mode transition in a sequential parallel turbocharged automotive diesel engine. *Int. J. Automotive Technology* **10**, **2**, 141−149.

Gautier, P., Albrecht, A. and Chasse, A. (2009). A simulation study of the impact of LP EGR on a two-stage turbocharged diesel engine. *Oil & Gas Science and Technology* **64** , **3**, 361−379.

GT-SUITE (2008). Flow Theory Manual. Chapter3: Turbines, Compressors and Boosting. Version7.2. Gamma Technologies.

Inman, S., Haworth, D. and El-Gindy, M. (2002). *Integration of WAVE and Advisor Simulations for Optimization of a Hybrid Electric Sport Utility Vehicle*. Pennsylvania State University. The Graduate School. College of Engineering.

Jung, M. (2003). *Mean-value Modeling and Robust Control of the Airpath of a Turbocharged Diesel Engine*. Ph.D. Dissertation. Cambridge University. Cambridge.

U.K.

Kao, Minghui and Moskwa, J. J. (1995). Turbocharged diesel engine modeling for nonlinear engine control and state estimation. *Trans. ASME J. Dynamics Systems, Measurements and Control*, **117**, 1−11.

Kulkarni, M. M., Sinha, R. P. and Dhaliwal, H. C. (1992). Reduced order model of turbocharged diesel engine. *Proc. 1992 American Control Conf.*, **2**, 927−931.

Lee, J. (2012). Sliding mode observer for exhaust pressure estimation in light-duty diesel engines equipped with VGT and EGR system. *KSAE 2012 Annual Conf. and Exhibition Proc*., 31−36.

Moskwa, J. J. and Hedrick, J. K. (1992). Modeling and validation of automotive engines for control algorithm development. *Trans. ASME J. Dynamic Systems, Measurements and Control*, **114**, 228–285.

Olivier, G. and Philippe, M. (2009). Control of a turbocharged diesel engine fitted with high pressure and low pressure exhaust gas recirculation systems. *Joint 48th IEEE Conf. Decision and Control and 28th Chinese Control Conf.*, 6582−6589.

Park, J., Lee, K. S., Song, S. and Chun, K. M. (2010). Numerical study of a light-duty diesel engine with a dual-loop EGR system under frequent engine operating conditions using the DOE method. *Int. J. Automotive Technology* **11**, **5**, 617−623.

Pfeifer, A., Smeets, M., Herrmann, H.-O., Tomazic, D. R., Felix, R. and Schlober, A. (2002). A new approach to boost pressure and EGR rate control development for HD truck engines with VGT. *SAE Paper No*. 2002-01-0964.

Shamma, J. S. and Athans, M. (1991). Guaranteed properties of gain scheduled control for linear parameter-varying plants. *Automatica* **27**, **3**, 559−564.

Stefanopoulou, A. (2004). Pressure and temperature-based adaptive observer of air charge for turbocharged diesel engines. *Int. J. Robust and Nonlinear Control* **14**, **6**, 543− 560.

Storset, O. F. and Stefanopoulou, A. and Smith, R. (2000). Air charge estimation for turbocharged diesel engines. *Proc. American Control Conf.*, **1**, 39−44.

Swartling, F. (2005). *Gas Flow Observer for Diesel Engine with EGR*. M.S. Thesis. Vehicular Systems, Dept. Electrical Engineering at Linkõpings Universitet.

Upadhyay, D. (2001). *Modeling and Model Based Control Design of the VGT-EGR System for Intake Flow Regulation in Diesel Engines*. Ph.D. Dissertation. The Ohio University.

Wang, J. (2008). Air fraction estimation for multiple combustion mode diesel engines with dual-loop EGR systems. *Control Engineering Practice*, **16**, 1479−1486.

Zheng, Q. (1999). *Modeling and Control Issues with Neutral Idle Shift in Transmissions*. Ph.D. Dissertation. The Ohio-State Univerisity.